

铝热反应法制备双股类螺旋 Zn_2SnO_4 单晶纳米带

王煜¹ 陈静¹ 廖清² 孙伟¹ 厉建龙^{1,*} 张建平³ 吴凯^{1,*}
(¹北京大学化学与分子工程学院, 北京分子科学国家实验室, 北京 100871; ²中国科学院化学研究所, 北京 100190; ³中国人民大学化学系, 北京 100872)

Bifilar Helix-Like Nanobelt of Single Crystalline Zn_2SnO_4 Fabricated by Aluminothermal Reaction Approach

WANG Yu¹ CHEN Jing¹ LIAO Qing² SUN Wei¹ LI Jian-Long^{1,*}
ZHANG Jian-Ping³ WU Kai^{1,*}

(¹Beijing National Laboratory for Molecular Sciences, College of Chemistry and Molecular Engineering, Peking University, Beijing 100871, P. R. China; ²Institute of Chemistry, Chinese Academy of Sciences, Beijing 100190, P. R. China; ³Department of Chemistry, Remin University of China, Beijing 100872, P. R. China)

*Corresponding authors. WU Kai, Email: kaiwu@pku.edu.cn; Tel: +86-10-62754005.
LI Jian-Long, Email: jlipku@pku.edu.cn; Tel: +86-10-62757062.

Part 1: Collection of the final products.

In order to clarify the distribution of the finally collected products, a schematic drawing of the collector geometry is given in Fig.S1a. In our experiments, we found that most of the Si wafer surface was covered with BHZN, as shown by the SEM (Fig.1 in the main context) and XRD data (Fig.S1b) of the as-prepared sample. Generally, the red zone in Fig.S1a was mainly covered by ZnO and the blue zones, mainly by Zn₂SnO₄. However, the Zn₂SnO₄ product could be mixed with a small amount of ZnO.

Part 2: Lattice structure of the bifilar helix-like Zn₂SnO₄ nanobelt

A particular bifilar helix-like Zn₂SnO₄ nanobelt (BHZN, Fig.S2a) was chosen for detailed structural analyses. Both ED along the [011] direction (Fig.S2b) and HRTEM images (Figs.S2c – h) and their corresponding Fourier transforms (Insets in Figs.S2c - h) at different spots along the BHZN showed that the BHZN was single crystal in nature. Its axis was along the $[\bar{1}11]$ direction. The lattice dislocations in Figs.S2c, e and h substantiate that the BHZN was indeed composed of two individual ZTO nanobelts.

Part 3: Role of the Au particles and identification of single zigzag ZTO nanobelt

Without the Au layer on Si wafer, no BHZNs were synthesized under our experimental conditions. On the other hand, under the same experimental conditions without the precursors, the Au layer on the Si wafer shrank into many small nanoparticles ranging from 60 to 80 nm in diameter (Fig.S3a), in fairly good agreement with the Au size detected at the BHZN end shown in Fig.3e. If we put the precursors in and raised the temperature to 950 °C in 50 min in 80 cm³·min⁻¹ N₂ and 20 cm³·min⁻¹ Ar and then immediately cooled the sample down to RT without dwelling, produced were some short nanowires on top of which the Au particles were seated (Fig.S3b). This supports the VLS growth mechanism. If the sample in the experiment for Fig.S3b dwelt for 30 min, then single zigzag ZTO nanobelt was fabricated (Figs.S3c and S3d), showing that the turbulent flow accelerated the formation of the zigzag nanobelt.

Part 4: Role of the gas flow

If a gas reservoir was added in between the 3-way gas valve and the CVD device, either only flat nanobelts were produced whose ends were bent a little bit at a molar ratio of 1:2:12 for ZnO:SnO₂:Al (Figs.S4a and S4b) or pyramid-composed nanowire (indicated by the arrow in Fig.S4c) as reported in Ref. 10f and single twisted nanobelt (as pointed out by the arrow in Fig.S4d) were synthesized at a molar ratio of 1:4:12 for ZnO:SnO₂:Al. The latter two structures might be caused by non-steady-state gas flow in the CVD device. Nonetheless, these results again substantiated that no BHZNs could be produced without the steady-state turbulent gas flow.

Part 5: Existence of ZnO nanobelts

Under our preparation conditions, a few of ZnO nanobelts could co-exist with the BHZN. Since the Zn and Sn vapors had a vapor pressure gradient along the CVD tube axis, ZnO nanobelts could distribute on Si wafer even the device temperature was kept at 950 °C. Fig.S5 shows the products at about 3 mm in front of the central part (where BHZNs were normally collected) of the Si wafer. Some ZnO nanobelts can be clearly observed in Fig.S5a. Fig.S5b is the EDX analysis of a single ZnO nanobelt in TEM measurement, which clearly indicates that ZnO is the chemical composition. This is why in our PL experiments ZnO emission feature appeared in the PL spectroscopy.

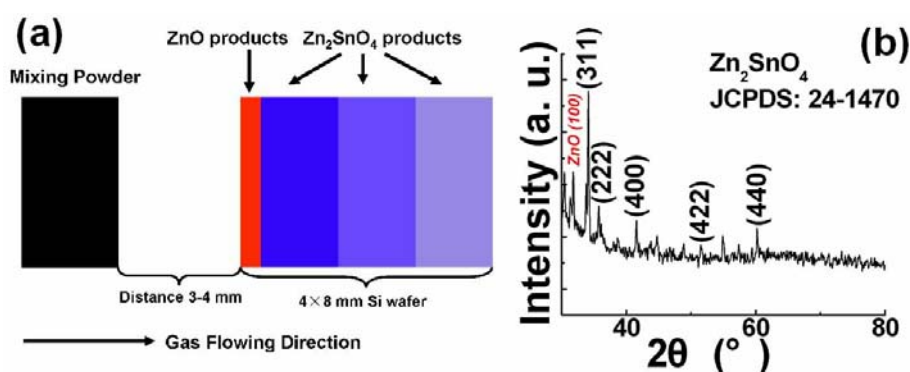


Fig.S1 (a) Schematic drawing of the collection geometry of the final products on the Si wafer. In the red zone, the main product was ZnO. In the blue areas, the main product was Zn₂SnO₄. The paler the blue color, the lower the concentration of the Zn₂SnO₄ per unit area. Therefore, most of the Si wafer surface was covered with BHZN. (b) XRD data of the as-prepared sample showing the main Zn₂SnO₄ product mixed with some ZnO.

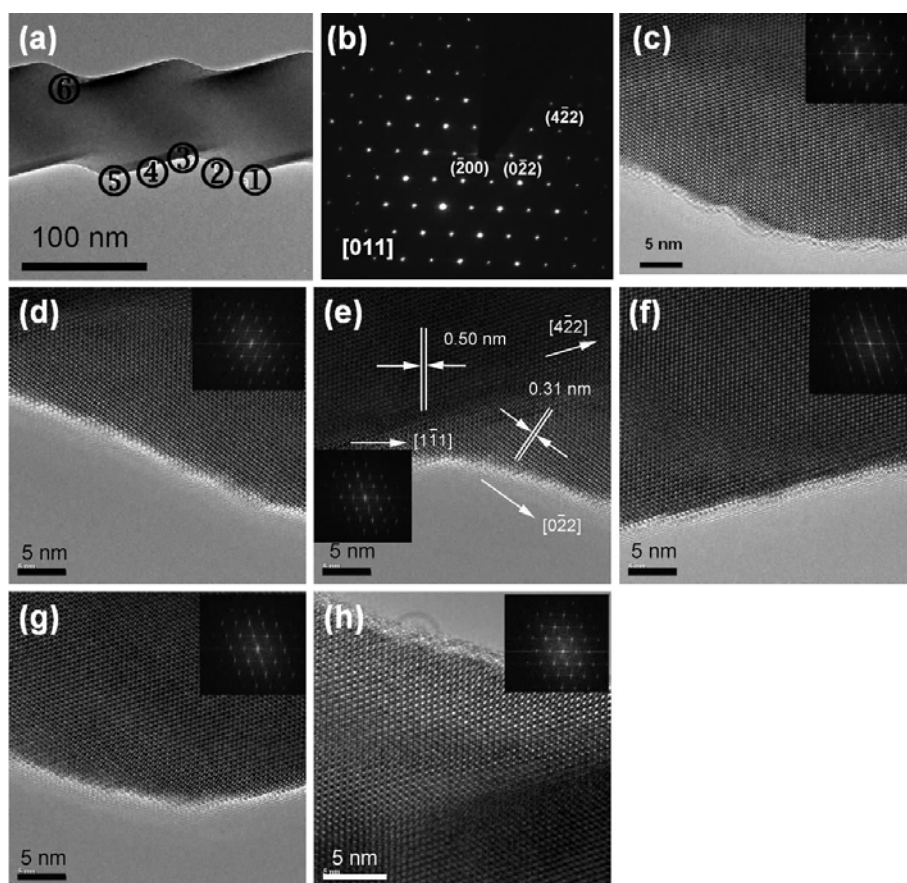


Fig.S2 (a) TEM of a BHZN. (b) ED pattern along the $[011]$ direction, which is the opposite direction of $[0\bar{1}\bar{1}]$ shown in Figs.1c and 1d in the main context. (c) - (h) HRTEM images sampled at the corresponding spots numbered 1 through 6 in (a). Insets in (c) - (h) are the Fourier transforms of the corresponding HRTEM images.

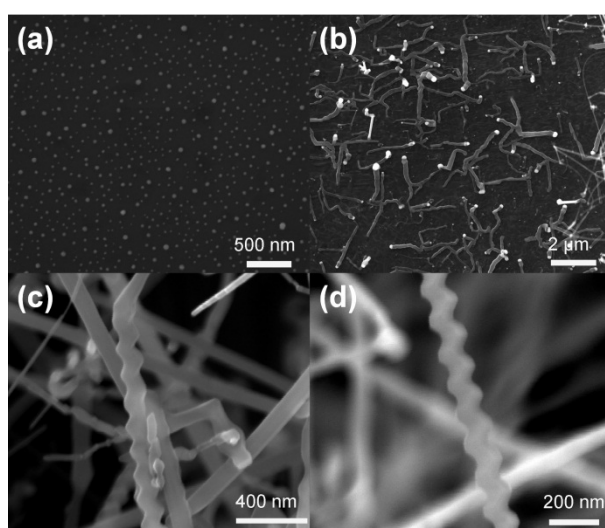


Fig.S3 (a) SEM image of Au nanoparticles produced on the Si wafer treated at 950 °C in $30 \text{ cm}^3 \cdot \text{min}^{-1} \text{ N}_2$ without precursors placed in the CVD. (b) SEM image of the

nanostructures produced with the precursors placed in CVD and after temperature rise to 950 °C and swift cooling down to room temperature. (c) and (d) SEM Images of the zigzag structures synthesized under the same experimental conditions for the samples 1a and 1b.

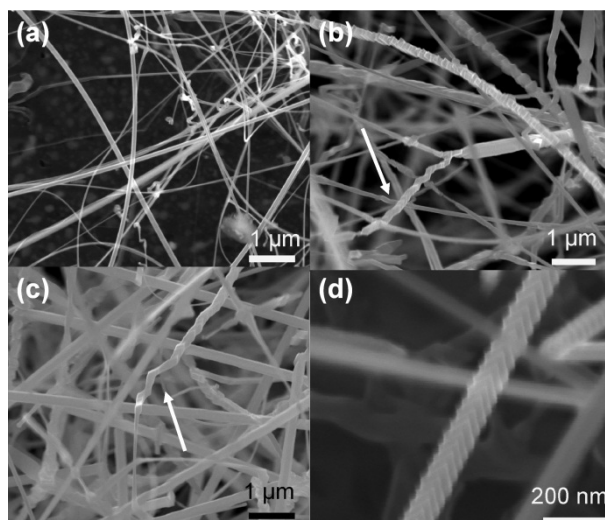


Fig.S4 Experimental results when a gas reservoir was added in between the 3-way gas valve and the CVD device. SEM images of the as-prepared products on Si wafer at a molar ratio of 1:2:12 [(a) and (b)], and 1:4:12 [(c) and (d)] for the mixed ZnO:SnO₂:Al precursors.

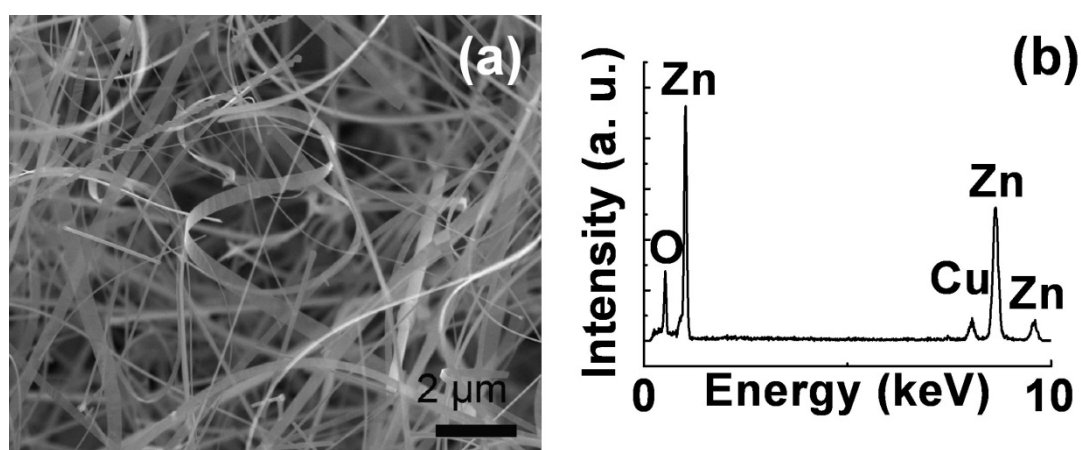


Fig.S5 (a) SEM of the ZnO nanobelts collected in the red zone at the Si wafer in Fig.S1a and (b) the corresponding EDX analysis of a single ZnO nanobelt in TEM.